

Cite this: *RSC Adv.*, 2019, 9, 11670

Preparation of thin solid electrolyte by hot-pressing and diamond wire slicing

 Masashi Kotobuki,^{ab} Houhua Lei,^c Yu Chen,^{bd} Shufeng Song,^e
 Chaohe Xu,^e Ning Hu,^e Janina Molenda^f and Li Lu^{*ab}

The thickness of a solid electrolyte influences the performance of all-solid-state batteries due to increased impedance with a thick electrolyte. Thin solid electrolytes are favourable to improve the performance of all-solid-state batteries due to the short Li ion diffusion path and small volume of the solid electrolytes. Therefore, the preparation of thin solid electrolyte is one of the key process techniques for development of all-solid-state batteries. In this study, thin $\text{Li}_{1.5}\text{Ge}_{1.5}\text{Al}_{0.5}(\text{PO}_4)_3$ solid electrolyte with a Na super ion conductor structure is prepared by diamond wire slicing. The $\text{Li}_{1.5}\text{Ge}_{1.5}\text{Al}_{0.5}(\text{PO}_4)_3$ solid electrolyte is prepared by melt-quenching followed by crystallization at 800 °C for 8 h, after which the crystallized $\text{Li}_{1.5}\text{Ge}_{1.5}\text{Al}_{0.5}(\text{PO}_4)_3$ rod is subjected to wire slicing. Thin $\text{Li}_{1.5}\text{Ge}_{1.5}\text{Al}_{0.5}(\text{PO}_4)_3$ with a thickness of 200 μm is obtained. The crystal structure and cross-sectional morphology are not affected by the slicing. The total Li conductivity of the thin $\text{Li}_{1.5}\text{Ge}_{1.5}\text{Al}_{0.5}(\text{PO}_4)_3$ and activation energy are $3.3 \times 10^{-4} \text{ S cm}^{-1}$ and 0.32 eV, respectively. The thickness and total conductivity are comparable to those of $\text{Li}_{1.5}\text{Ge}_{1.5}\text{Al}_{0.5}(\text{PO}_4)_3$ prepared by the tape-casting method which needs several steps to prepare $\text{Li}_{1.5}\text{Ge}_{1.5}\text{Al}_{0.5}(\text{PO}_4)_3$ tape-sheet and high temperature and a long sintering process. The ionic transference number of the thin $\text{Li}_{1.5}\text{Ge}_{1.5}\text{Al}_{0.5}(\text{PO}_4)_3$ is 0.999. The diamond wire slicing is a useful method to prepare thin solid electrolytes.

Received 26th January 2019
Accepted 5th April 2019

DOI: 10.1039/c9ra00711c

rsc.li/rsc-advances

1. Introduction

The current commercial Li-ion batteries use highly ionic conductive organic electrolytes, which has brought a lot of convenience in cell fabrication and at the same time also causes serious safety issues, such as electrolyte leakage and fire hazard due to the use of flammable organic solvents.^{1,2} All-solid-state batteries with non-flammable ceramic electrolytes are expected to solve the safety problems.^{3–5} Therefore, many kinds of solid electrolytes such as garnet,^{6–8} perovskite,^{9–11} and NASICON-types^{12,13} have been intensively researched and developed due to their reasonably high Li ion conductivities. Among them, LAGP ($\text{Li}_{1+x}\text{Al}_x\text{Ge}_{2-x}(\text{PO}_4)_3$, $0 \leq x \leq 0.7$) with a NASICON structure is of particular interest due to its high Li ion conductivity and wide electrochemical window.^{14–16}

In an all-solid-state battery, the thickness of the solid electrolyte influences the performance as schematically illustrated in Fig. 1. The purpose of an electrolyte in a battery is to prevent short circuit between the positive and negative electrodes but allow Li ions to transfer from the anode to the cathode during discharge and *vice versa*. Since Li ion migration between the two electrodes is a diffusion process, a thick solid electrolyte will lead to an increase in impedance of the all-solid-state battery and hence difficulties of charge transfer. Additionally, the electrolyte is an inactive material, and a large volume of the thick electrolyte implies a lower volumetric and gravimetric power and energy densities.¹⁷ Therefore, process techniques to prepare thin and dense solid electrolyte are essential.

For preparation of thin solid electrolytes, physical vapour processes such as sputtering and PLD (pulse laser

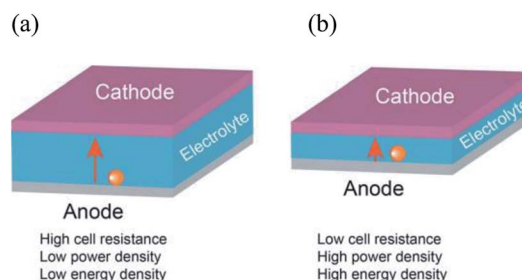


Fig. 1 Performances of all-solid-state batteries with (a) thick and (b) thin solid electrolytes.

^aDepartment of Mechanical Engineering, National University of Singapore, 9 Engineering Drive 1, Singapore 117576, Singapore. E-mail: lluli@nus.edu.sg

^bNational University of Singapore Suzhou Research Institute, Dushu Lake Science and Education Innovation District, Suzhou 215123, P. R. China

^cSolid-Force Pte. Ltd., Dushu Lake Science and Education Innovation District, Suzhou 215123, P. R. China

^dSchool of Optoelectronic Science and Engineering, Collaborative Innovation Centre of Suzhou Nano Science and Technology, Soochow University, Suzhou 215006, China

^eCollege of Aerospace Engineering, Chongqing University, Chongqing, 400044, P. R. China

^fAGH University of Science and Technology, Faculty of Energy and Fuels, Mickiewicz 30, 30-059 Krakow, Poland



deposition)^{18,19} and liquid processes like the sol-gel method²⁰ have been studied. However, these physical processes have some disadvantages such as usage of vacuum system, difficulty in control of chemical composition and large area coating. Also, in both processes, the thin solid electrolytes must be deposited on a substrate and it is difficult to obtain self-standing thin electrolytes. Although a simple method to obtain the self-standing thin solid electrolytes is to grind a thick solid electrolyte pellet to a thin one, this process is time-consuming and easy to create defect. Imanishi *et al.* applied the tape-casting method for preparation of thin LAGP solid electrolyte²¹ and obtained thin LAGP with a thickness of 228 μm . Using this processing, a total conductivity $3.38 \times 10^{-4} \text{ S cm}^{-1}$ was achieved.²² This verified the tape-casting method was useful for thin solid electrolyte preparation, however, the tape-casting method has a number of drawback, including complexity of processing and composition deviation from desired one.

To obtain the self-standing thin electrolytes, the simple slicing technique using a diamond saw is considered to be useful and was applied for the garnet-type solid electrolytes,^{23,24} however, the diamond saw slicing tends to form kerf and waste materials. Contrary, the diamond wire slicing using a wire impregnated with diamond dust produces less kerf and wasted materials compared with the diamond saw slicing. Additionally, the diamond wire slicing is also practical and less expensive process.²⁵

In this study, the diamond wire slicing was applied for LAGP solid electrolyte first time. By the diamond wire slicing of thick LAGP pellet, thin LAGP slices of a thickness of about 200 μm can be successfully prepared.

2. Experimental

2.1 Preparation of LAGP solid electrolyte

In order to slice the LAGP solid electrolyte, thick LAGP rod with a length of about 2 cm was needed. In a typical processing, the LAGP rods were prepared by melt-quenching method followed by hot-press technique.²⁶ The precursors of Li_2CO_3 (>99.99%), GeO_2 (>99.999%), Al_2O_3 (99.98%) and $\text{NH}_4\text{H}_2\text{PO}_4$ (>98%) which were all purchased from Sigma Aldrich were mixed in ethanol, dried and heated at 380 $^\circ\text{C}$ for 2 h in an Al crucible. To compensate Li evaporation, 10 mol% excess Li_2CO_3 was added. After grinding, the obtained powder was melted in a Pt crucible at 1350 $^\circ\text{C}$ for 2 h and casted on a stainless plate pre-heated at 500 $^\circ\text{C}$. After solidification, the cast glass was annealed at 500 $^\circ\text{C}$ for 2 h to release the thermal stress. The glass was crushed into powder. The crushed glass powder was loaded into a graphite die of 10 mm in a diameter and then subjected to hot-press sintering.²⁷ Since glass transition temperature, T_g , and crystallization temperature, T_c , are 530 and 603 $^\circ\text{C}$, respectively,²⁷ to fully utilize rubber-like behaviour, the glass powder was hot-pressed at 600 $^\circ\text{C}$ under a pressure of 20 MPa for 1 h in an Ar atmosphere. After hot-press sintering, the sintered-glass was crystallized at 800 $^\circ\text{C}$ for 8 h in a heating rate of 3 $^\circ\text{C min}^{-1}$ in air and under atmospheric pressure to obtain crystallized LAGP. This batch sample is denoted as sample 1. For a comparison, the hot-press sintered-glass without crystallization was also

prepared. This batch of samples was crystallized in same condition after slicing and denoted as sample 2 as shown in Fig. 2.

2.2 Slicing LAGP solid electrolyte

As a tradition processing, a diamond wire was used to slice the rod. To avoid heat effect, aqueous lubricant coolant was used during whole slicing process. The slicing rate was adjusted to about 0.1 mm min^{-1} .

2.3 Characterization

As a crystal structure of the thin LAGP was identified by XRD measurement (XRD-6000, Shimadzu) with Cu K_α radiation from $2\theta = 10$ to 60° with a step of 0.02° at a scan rate of 1° min^{-1} . Microstructure and morphology of the thin LAGP solid electrolytes was observed by scanning electron microscope (SEM, JEOL-6010 PLUS/LV) operating at 15 kV. Au was sputtered on the samples to add an electronic conductivity and eliminate the charge effect. Densities of the thin LAGP solid electrolytes were measured by using a pycnometer (AccuPyc II 1340, Micromeritics).

The Li ion conductivity of the thin LAGP was estimated by the electrochemical impedance spectroscopy method. Prior to measurement, Au was sputtered on both surfaces of the samples to prepare the Li ion blocking electrodes and ensure electrical contact. The impedance measurement was performed at a voltage signal of 10 mV in a frequency range of 10–1 MHz at 28–150 $^\circ\text{C}$ using a Solartron impedance analyser 1470E cell test system. The activation energy was calculated from Arrhenius plot using following equation.

$$\sigma_t = A \exp(-E_a/k_B T) \quad (1)$$

where σ_t , E_a , k_B , A and T are total Li ion conductivity, activation energy, Boltzmann constant, pre-exponential factor and absolute temperature, respectively.

Ionic transference number of the thin LAGP solid electrolyte was measured by DC polarization technique.²⁸ A DC voltage of 1.0 V was applied to the Au/LAGP/Au cell. The ionic transference number (t_i) was calculated from initial current, I_i and stabilized current, I_f , using following equation:

$$t_i = \frac{I_i - I_f}{I_i} \quad (2)$$

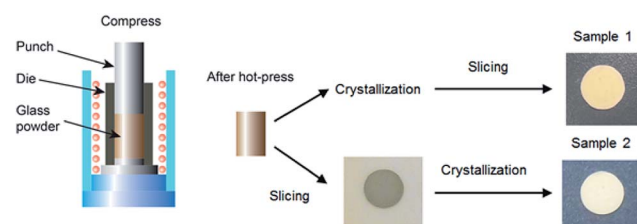


Fig. 2 A scheme of preparation of thin LAGP by the diamond wire slicing.



3. Results and discussion

3.1 Characterization of thin LAGP solid electrolyte

Fig. 3 shows images of the thin LAGP pellets. For the sample 1, the white coloured thin pellet with 200 μm in a thickness was obtained. In the diamond saw slicing of garnet-type electrolytes, thicknesses of pellets were almost same (0.18–0.22 cm).^{23,24} For the sample 2, the thin pellet with grey colour was changed into white colour through the crystallization. The thickness of the sample 2 before the crystallization was 290 μm . The thickness became slightly smaller due to shrinkage during the crystallization, while diameter of the sample 2 did not change through the crystallization.

XRD patterns of the thin LAGP pellets were depicted in Fig. 4a. In both samples, main phase could be attributed to LAGP with NASICON structure. Also, small peaks of GeO_2 and $\text{Al}_6\text{Ge}_2\text{O}_{13}$ was also observed in both diffraction patterns. Table 1 reveals lattice parameters of the sample 1 and 2. For a comparison, LAGP solid electrolyte crystallized at same temperature without the slicing is also shown in Table 1.²⁶ The sample 1 possessed slightly larger lattice parameter in a-axis than that of the sample without slicing, whereas c-axis of the sample 1 was much shorter. For the sample 2, a-axis was shorter than that of others, while c-axis of the sample 2 was a little longer than the sample 1 and much shorter than the sample without slicing. As a result, the lattice volume of the sample 1 was larger than that of the sample 2 and smaller than that of the sample without slicing. This observation implied that the sample preparation history influenced lattice parameters. The influence of the sample history on the properties of samples was shown more clearly in morphological observation.

Fig. 4b shows cross-sectional SEM images of the sample 1 and 2. For the sample 1 (Fig. 4b(1) and (2)), many densely packed small crystal grains whose sizes were about 2 μm , were observed. No porosity was noted. These morphological features were very similar to the sample without slicing.²⁶ In contrary, the sample 2 (Fig. 4b(3) and (4)) showed different cross-sectional morphologies. Crystal grains showed non-uniform size ranging from 100 nm to >10 μm .

Additionally, there were some pores in the cross-section. It was also noted that there was a large difference in the relative density. The relative densities of the sample 1 and 2 are 98.9 and 88.7%, respectively. We studied history of the processing and

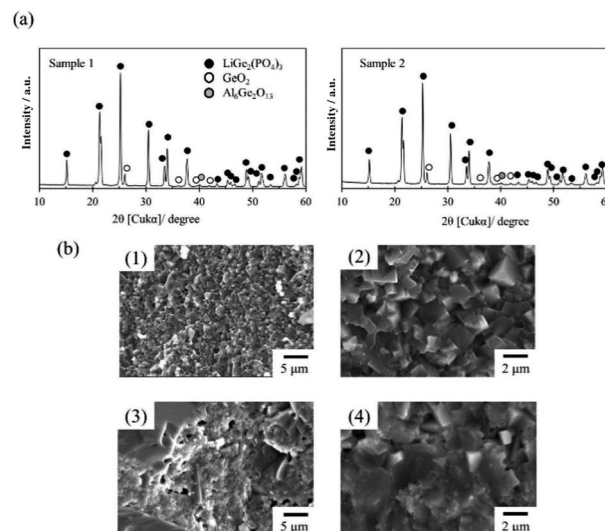


Fig. 4 (a) XRD patterns of sample 1 and sample 2, (b) cross-sectional SEM images of (1 and 2) sample 1 and (3 and 4) sample 2.

noted that the hot-pressing was carried out at the temperature between T_g and T_c where the glass powder showed a rubber-like behaviour. Therefore, it is easy to achieve a very dense pellet even at 20 MPa as illustrated in Fig. 5(a). However, although the glass powder could be hot-pressed to almost no porosity, powder particles were roughly bonded mechanically since low pressing temperature and short pressing duration would be unable to achieve sufficient chemical bonding. A good chemical bonding was achieved at 800 $^{\circ}\text{C}$ during the crystallization (Fig. 5(b1)). Since a good bonding was obtained in the crystallization process, dense thin slices with no or little damage could be obtained (Fig. 5(c1)). However, if the slicing was carried out directly after hot-pressing, cleavage crack and impact from the diamond wire could cause delamination and crack as shown in Fig. 5(b2). The delamination and cracks would be further expanded due to shrinkage during post-crystallization process (Fig. 5(c2)).

3.2 Electrochemical properties of thin LAGP solid electrolyte

The Li ion conductivity of the thin LAGP samples was evaluated by the electrochemical impedance method. Fig. 6 depicts impedance spectra of the sample 1 and 2 measured at 28 $^{\circ}\text{C}$. In both spectra, a semicircle and a tail were observed in the high- and low-frequency range, respectively. This characteristic profile of the impedance plot often appears in ceramics that are

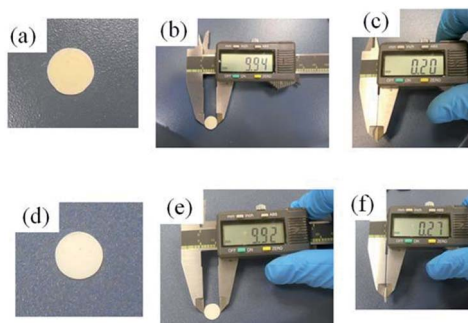


Fig. 3 Photos and dimensions of (a–c) sample 1 and (d–f) sample 2.

Table 1 Lattice parameters of thin LAGP prepared by mechanical slicing^a

Sample	a (\AA) (± 0.002)	c (\AA) (± 0.002)	V (\AA^3) (± 0.4)
Thick LAGP	8.262	20.656	1221.0
Sample 1	8.265	20.619	1219.8
Sample 2	8.255	20.624	1217.0

^a Ref. 26.



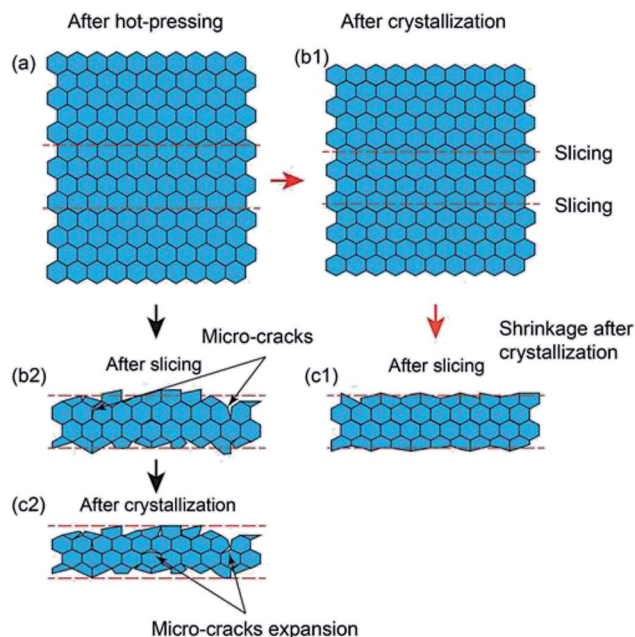


Fig. 5 Schematic illustration on difference of sample morphologies in the history of processing.

ion conductive.^{29,30} The tail corresponds to capacitive blocking behaviour of the electrodes.³¹

The intercepts of the semicircle at the high- and low-frequency sides are assigned to inner crystal and total (inner crystal and grain boundary) impedances, respectively. Estimated bulk (inner crystal) and total conductivities of the sample 1 were 5.9×10^{-4} and $3.3 \times 10^{-4} \text{ S cm}^{-1}$, respectively. Imanishi *et al.* prepared thin LAGP with a thickness of 228 μm and reported its total conductivity was $3.38 \times 10^{-4} \text{ S cm}^{-1}$.²² Although the thickness and total conductivity were comparable to those of the sample 1, the diamond wire slicing can simplify the

preparation process significantly. Fig. 7 reveals a comparison experimental procedures of tape-casting and mechanical slicing methods. The tape-casting method requires many steps including twice long ball-milling processes. Contrary, this diamond wire slicing needs only 4 steps to obtain thin LAGP. This simple technique can reduce not only time and energy for thin LAGP preparation, but also production cost. In the sample 2, a depressed semicircle was observed. This would be because grain boundaries were non-uniform due to uneven growth of crystal grains. The bulk and total conductivities of the sample 2 were 1.5×10^{-4} and $1.2 \times 10^{-4} \text{ S cm}^{-1}$, respectively. Both conductivities were lower than those of the sample 1 due to pores, non-uniform crystal grains and poor bonding.

Based on temperature dependence of the Li ion conductivities, activation energy of the sample 1 was calculated. Above 75 $^{\circ}\text{C}$, the bulk and total impedances could not be separated due to a disappearance of the semicircle. Therefore, only total conductivity was used for the activation energy calculation. The Arrhenius plot (Fig. 8a) could be fitted by a straight line and hence the activation energy was calculated to be 0.32 eV from slope of the straight line. This value is same as that of tape-casting LAGP (0.32 eV).²²

Ionic transference number of the sample 1 was examined using Au/LAGP/Au cell by the DC polarization technique. The polarization curve is shown in Fig. 8b. The ionic transference number can be calculated by the initial and stabilized current. The calculated ionic transference number is >0.999 , indicating that the sample 1 is a pure ionic conductor.

It is verified that the diamond wire slicing is a very simple and useful method to obtain thin solid electrolytes. In this study, the hot-press was used to prepare thick LAGP rod, however, conventional sintering method also can be used if thick rod could be obtained. Additionally, this slicing technique can be applied for other solid electrolytes such as garnet- and perovskite-type solid electrolytes. Furthermore, by optimization of slicing condition, thinner solid electrolyte would be obtained. These attempts are being studied in our group. The results will be reported in due course.

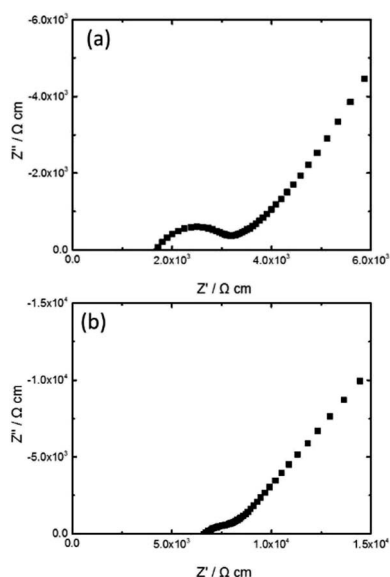


Fig. 6 Complex impedance plots of (a) sample 1 and (b) sample 2 measured at 28 $^{\circ}\text{C}$ in a voltage signal of 10 mV.

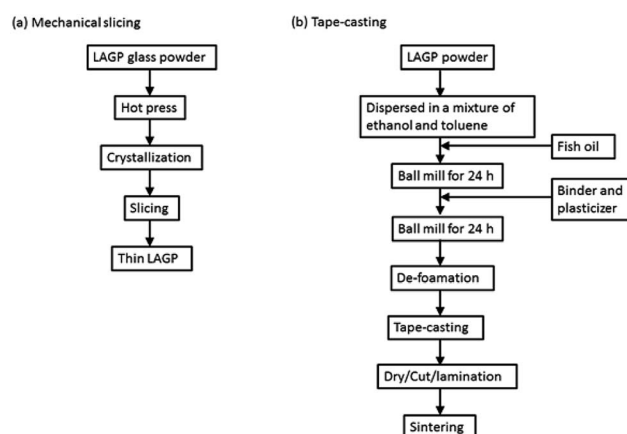


Fig. 7 A comparison of experimental procedures of (a) diamond wire slicing and (b) tape-casting methods.²²



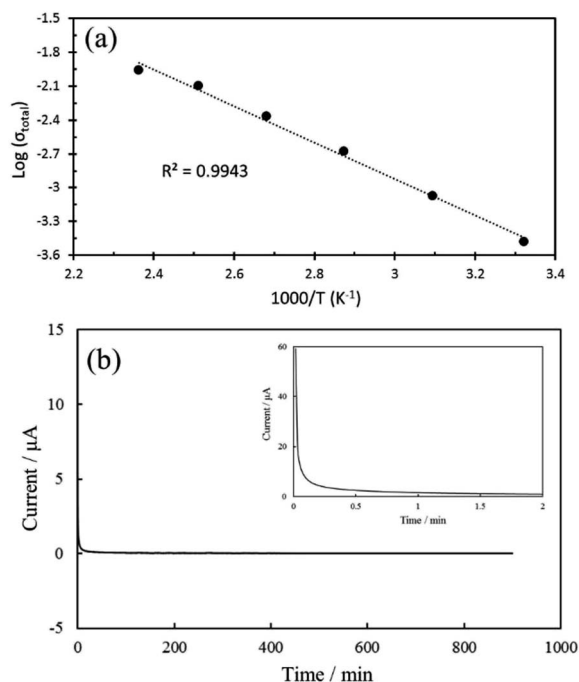


Fig. 8 (a) Arrhenius plot of total Li ion conductivity of sample 1 and (b) chronoamperometric curve of the sample 1 measured at an applied voltage of 1 V.

4. Conclusions

Thin LAGP solid electrolyte was prepared by hot-pressing and simple diamond wire cutting. Two kinds of samples were fabricated for the cutting: one was crystallized LAGP and another one was glass LAGP. The glass LAGP was crystallized after the slicing. Both samples revealed very similar XRD patterns in which main phase was LAGP with NASICON structure, while morphology was very different. The sample sliced after the crystallization showed uniformly grown crystal grains with about 2 μm in size and no gap among the crystal grains. In contrary, the sample crystallized after the slicing exhibited non-uniform crystal growth. Sizes of crystal grains were a range from 100 nm to >10 μm . Additionally, there were some pores in the cross-section. As a result, the sample sliced after crystallization revealed higher bulk and total Li ion conductivities, 5.9×10^{-4} and $3.3 \times 10^{-4} \text{ S cm}^{-1}$ in a thickness of 200 μm , respectively. The thickness and Li ion conductivity were comparable to LAGP prepared by the tape-casting method which needs several steps to prepare LAGP tape-sheet and high temperature and long sintering process. The diamond wire slicing is a simple and useful method to obtain thin solid electrolytes. Thinner solid electrolyte would be obtained by optimization of slicing conditions.

Conflicts of interest

There are no conflicts to declare.

Acknowledgements

This work is supported by National University of Singapore, National University (Suzhou) Research Institute, Solid-Force Pte

Ltd (Suzhou, China), the National Natural Science Foundation of China (NSFC 51572182, 11502036, 11372104, 11632004), the Natural Science Fund of the city of Chongqing (cstc2015jcyjA0577), and the Key Program for International Science and Technology Cooperation Projects of the Ministry of Science and Technology of China (No. 2016YFE0125900).

Notes and references

- 1 Z. Feng, M. Kotobuki, S. Song, M. O. Lai and L. Lu, *J. Power Sources*, 2018, **389**, 198–213.
- 2 K. Hoshina, K. Yoshima, M. Kotobuki and K. Kanamura, *Solid State Ionics*, 2012, **209–210**, 30–35.
- 3 M. Kotobuki, Y. Isshiki, H. Munakata and K. Kanamura, *Electrochim. Acta*, 2010, **55**, 6892–6896.
- 4 A. A. Raskovalov, E. A. Il'ina and B. D. Antonov, *J. Power Sources*, 2013, **238**, 48–52.
- 5 S. Song, Z. Dong, F. Deng and N. Hu, *Funct. Mater. Lett.*, 2018, **11**, 1850039.
- 6 M. Kotobuki and M. Koishi, *Ceram. Int.*, 2014, **40**, 5043–5047.
- 7 M. Kotobuki, S. Song, R. Takahashi, S. Yanagiya and L. Lu, *J. Power Sources*, 2017, **349**, 105–110.
- 8 S. Qin, X. Zhu, Y. Jiang, M. Ling, Z. Hu and J. Zhu, *Funct. Mater. Lett.*, 2018, **11**, 1850029.
- 9 M. Kotobuki, Y. Suzuki, K. Kanamura, Y. Sato, K. Yamamoto and T. Yoshida, *J. Power Sources*, 2011, **196**, 9815–9819.
- 10 S. Stramare, V. Thangadurai and W. Weppner, *Chem. Mater.*, 2003, **15**, 3974–3999.
- 11 J. Wu, L. Chen, T. Song, Z. Zou, J. Gao, W. Zhang and S. Shi, *Funct. Mater. Lett.*, 2017, **10**, 1730002.
- 12 M. Kotobuki and M. Koishi, *Ceram. Int.*, 2013, **39**, 4645–4649.
- 13 M. Kotobuki, M. Koishi and Y. Kato, *Ionics*, 2013, **19**, 1945–1948.
- 14 J. K. Feng, L. Lu and M. O. Lai, *J. Alloys Compd.*, 2010, **501**, 255–258.
- 15 M. Kotobuki and M. Koishi, *Ceram. Int.*, 2015, **41**, 8562–8567.
- 16 M. Kotobuki, E. Hanc, B. Yan, J. Molenda and L. Lu, *Ceram. Int.*, 2017, **43**, 12616–12622.
- 17 *Ceramic electrolytes for all-solid-state Li batteries*, ed. M. Kotobuki, S. Song, C. Chen and L. Lu, World Scientific Publishing Co. Pte. Ltd., 2018.
- 18 B. J. Hwang, C. Y. wang, M. Y. Cheng and R. Santhanam, *J. Phys. Chem. C*, 2009, **113**, 11373–11380.
- 19 N. Kuwata, R. Kumar, K. Toribami, T. Suzuki, T. Hattori and J. Kawamura, *Solid State Ionics*, 2006, **177**, 2827–2832.
- 20 K. Tadanaga, H. Egawa, A. Hayashi, M. Tatsumisago, J. Mosa, M. Aparicio and A. Duran, *J. Power Sources*, 2015, **273**, 844–847.
- 21 M. Zhang, K. Yakahashi, I. Uechi, Y. Takeda, O. Yamamoto, D. Im, D.-J. Lee, B. Chi, J. Pu, J. Li and N. Imanishi, *J. Power Sources*, 2013, **235**, 117–121.
- 22 M. Zhang, Z. Huang, J. Cheng, O. Yamamoto, N. Imanishi, B. Chi, J. Pu and J. Li, *J. Alloys Compd.*, 2014, **590**, 147–152.
- 23 V. Thangadurai and W. Weppner, *J. Solid State Chem.*, 2006, **179**, 974–984.
- 24 R. Murugan, V. Thangadurai and W. Weppner, *Angew. Chem., Int. Ed.*, 2007, **46**, 7778–7781.



- 25 https://en.wikipedia.org/wiki/Wire_saw.
- 26 Y. Zhu, Y. Zhang and L. Lu, *J. Power Sources*, 2015, **290**, 123–129.
- 27 B. Yan, Y. Zhu, F. Pan, J. Liu and L. Lu, *Solid State Ionics*, 2015, **278**, 65–68.
- 28 M. Kotobuki, L. Lu, S. V. Savilov and S. M. Aldoshin, *J. Electrochem. Soc.*, 2017, **164**(14), A3868–A3875.
- 29 V. Thangadura and W. Weppener, *J. Power Sources*, 2005, **142**, 339–344.
- 30 M. Kotobuki, K. Kanamura, Y. Sato, K. Yamamoto and T. Yoshida, *J. Power Sources*, 2012, **190**, 346–349.
- 31 A. Kubanska, L. Castro, L. Tortet, O. Schaef, M. Dolle and R. Bouchet, *Solid State Ionics*, 2014, **266**, 44–50.

